Virtual biomechanics: a new method for online reconstruction of force from EMG recordings

Aymar de Rugy, Gerald E. Loeb and Timothy J. Carroll

J Neurophysiol 108:3333-3341, 2012. First published 26 September 2012;
doi: 10.1152/jn.00714.2012

J Neurophysiol 108: 3333–3341, 2012.
First published September 26, 2012; doi:10.1152/jn.00714.2012.

Virtual biomechanics: a new method for online reconstruction of force from EMG recordings

Aymar de Rugy,[1] Gerald E. Loeb,[2] and Timothy J. Carroll[1]

[1]*Centre for Sensorimotor Neuroscience, School of Human Movement Studies, The University of Queensland, Brisbane, Australia; and* [2]*Department of Biomedical Engineering, University of Southern California, Los Angeles, California*

Submitted 17 August 2012; accepted in final form 23 September 2012

de Rugy A, Loeb GE, Carroll TJ. Virtual biomechanics: a new method for online reconstruction of force from EMG recordings. *J Neurophysiol* 108: 3333–3341, 2012. First published September 26, 2012; doi:10.1152/jn.00714.2012.—Current methods to reconstruct muscle contributions to joint torque usually combine electromyograms (EMGs) with cadaver-based estimates of biomechanics, but both are imperfect representations of reality. Here, we describe a new method that enables online force reconstruction in which we optimize a "virtual" representation of muscle biomechanics. We first obtain tuning curves for the five major wrist muscles from the mean rectified EMG during the hold phase of an isometric aiming task when a cursor is driven by actual force recordings. We then apply a custom, gradient-descent algorithm to determine the set of "virtual pulling vectors" that best reach the target forces when combined with the observed muscle activity. When these pulling vectors are multiplied by the rectified and low-pass-filtered (1.3 Hz) EMG of the five muscles online, the reconstructed force provides a close spatiotemporal match to the true force exerted at the wrist. In three separate experiments, we demonstrate that the technique works equally well for surface and fine-wire recordings and is sensitive to biomechanical changes elicited by a modification of the forearm posture. In all conditions tested, muscle tuning curves obtained when the task was performed with feedback of reconstructed force were similar to those obtained when the task was performed with real force feedback. This online force reconstruction technique provides new avenues to study the relationship between neural control and limb biomechanics since the "virtual biomechanics" can be systematically altered at will.

motor control; myoelectric control; biomechanics; reaching movements; sensorimotor transformation

EVEN SIMPLE MOVEMENTS REQUIRE the coordinated recruitment of multiple muscles. The net joint torques required to perform a movement can be computed from the observable kinematics by the method of inverse dynamics, but these torques might be achieved by many different combinations of individual muscle forces (Bernstein 1967). This is the so-called "redundancy problem," and how the central nervous system (CNS) selects specific patterns of muscle activation to perform a given task remains one of the most critical unresolved questions in motor control. Indeed, the ability to resolve redundancy is central to the attractiveness of several influential motor control schemes, including optimal control, motor primitives, and hierarchical sensorimotor control (e.g., d'Avella et al. 2003; Haruno and Wolpert 2005; Loeb et al. 1999; Todorov 2004; Todorov and Jordan 2002). Most previous approaches to test predictions of these theories involved observing how muscle activation patterns vary according to task under natural conditions. However, because of the high degree of correlation among muscle activation and limb kinetics and kinematics, many theoretical models might predict similar muscle activation solutions in a given natural situation. A more direct test of a particular hypothesis about the nature of the movement control system would be to see how it responds to changes in the musculoskeletal plant, which could be designed to probe and disambiguate solutions predicted by different theoretical models. Making such changes physically such as by surgical intervention is not ethical with human subjects. Furthermore, it tends to involve a prolonged recovery period, during which adaptations may be occurring but cannot be studied. In this paper, we present a virtual reality method in which subjects control an animated model of their musculoskeletal system in real-time by means of their electromyographic (EMG) signals.

There is extensive literature devoted to modeling methods that allow forward simulation of joint torques or kinematics from estimates of muscle activation. The approaches described previously vary from, at one extreme, models that seek to provide realistic simulations of the physiological processes of excitation-contraction coupling and the mechanical application of muscle forces to generate torques on the skeleton (e.g., Buchanan et al. 2004; Cheng and Loeb 2008; Erdemir et al. 2007; Tsianos et al. 2012) to approaches at the other extreme that are based purely on associations between measured EMG patterns and movement outcomes without consideration of muscle physiology or musculoskeletal mechanics (e.g., Seifert and Fuglevand 2002). Neither of these extreme approaches provides a method for the online reconstruction of joint torque from EMG records that is ideal for subsequent experimental manipulation according to our requirements. On the one hand, approaches based purely on statistical associations between muscle activation and movement outcomes provide no opportunity to manipulate specific aspects of the musculoskeletal plant. On the other hand, the accuracy of force reconstructions produced by a comprehensive neuromuscular-skeletal model remains contingent on accurate settings of the numerous parameters of such models, most of which are difficult to assess on an individual basis (e.g., Sartori et al. 2012). Furthermore, an ideal musculoskeletal model that perfectly represents a subject's biomechanics would still be insufficient to guarantee the quality of reconstructions because EMG records do not provide a perfectly accurate representation of muscle activation. For instance, EMG signals are subject to contamination by electrical activity of nearby muscles and represent only a fraction of all active motor units in the target muscle (Hug 2011; Staudenmann et al. 2010).

Address for reprint requests and other correspondence: A. de Rugy, Centre for Sensorimotor Neuroscience, School of Human Movement Studies, Rm. 424, Bldg. 26, Univ. of Queensland, St. Lucia QLD, 4072 Australia (e-mail: aymar@hms.uq.edu.au).

Because an accurate biomechanical model requires an accurate measurement of muscle activation for forward simulation of muscle force, and because the means to measure muscle activation accurately are unavailable, we designed a practical approach whereby a virtual representation of muscle biomechanics was defined that best reconstructs limb force when combined with EMG recordings. In this approach, the inaccuracy of the biomechanical representation is intended to compensate for imperfections of EMG recordings in a manner that best reconstructs force when both are combined. In separate experiments, we demonstrate that the technique works in different context of relatively low isometric force at the wrist joint, for which the EMG to force relationship is approximately linear. In particular, we show that the goodness of force reconstruction was similarly high for surface and fine-wire recordings, which are differentially affected by cross talk and vary in the degree to which they represent activity of the overall muscle. We also show that the technique is sensitive to biomechanical changes elicited by a modification of the forearm posture and is therefore suitable to address the important question of how the nervous system tunes motor commands to the biomechanics of the current posture (Buneo et al. 1997; Sergio and Kalaska 1997, 2003). Because it starts from the most intuitive relationship between muscle activity and force and enables virtual change in the biomechanics of any muscle, the technique offers novel opportunities to explore the nature of the adaptive controller embodied by the nervous system.

MATERIALS AND METHODS

Virtual Biomechanics

Overview. Fagg et al. (2002) proposed an optimal model that produces muscle activation patterns qualitatively similar to those observed experimentally for the biomechanics of a known muscle (Fig. 1*A*). Our virtual biomechanics technique consists in using a similar optimization procedure but in the opposite direction, i.e., to extract a representation of muscle biomechanics from observed muscle activations (Fig. 1*B*) and then combine the virtual biomechanics with real-time EMG to reconstruct force online (Fig. 2). First, we introduce the Fagg et al. (2002) model; second, we illustrate how using optimization in the reverse direction enables extraction of the virtual biomechanics from muscle activations; and third, we show how combining the virtual biomechanics with real-time EMG recordings enables accurate online force reconstruction.

The Fagg et al. (2002) model. For the biomechanics of a given muscle, Fagg et al. (2002) proposed a method to determine the overall activations of the various wrist muscles without requiring direct information such as EMG. It is based on the assumption that the CNS would minimize the summed squared activation across all muscles. In this model, the extrinsic direction of action (up/down and right/left) of each muscle i is defined by a two-element pulling vector, $\mathbf{P}_i$, and muscles contribute to the endpoint movement along their vector of action with a length proportional to their activation levels, a_i. The endpoint movement is described by the two-element vector $\mathbf{x}$:

$$\mathbf{x} = \sum_{i \in A} \mathbf{P}_i \, a_i$$

where A is the set of five muscles. The authors then consider the minimization of the following two criteria error function (endpoint error and muscle activation):

$$E = \frac{1}{2}\|\mathbf{x}_{targ} - \mathbf{x}\|^2 + \frac{\lambda}{2}\|\mathbf{a}\|^2$$

subject to $a_i \geq 0$ for all $i \in A$, where $\mathbf{x}_{targ}$ is a vector representing the target location, λ is a regularization parameter set to 0.02, $\mathbf{a}$ is the muscle activation vector, and $\|.\|$ denotes the magnitude of a vector. The authors showed that minimizing this cost function produced muscle activation patterns that were qualitatively similar to those observed experimentally in EMG recordings. In particular, these patterns exhibit a cosinelike recruitment of muscles as a function of movement directions and reproduce the observed discrepancies between directions for which muscles are preferentially used and their direction of action (Fig. 1).

Extracting muscle virtual biomechanics from EMG. Assuming that we know the muscle activation patterns (e.g., recorded experimentally) but not the biomechanics, we use optimization in the direction opposite to that used in the Fagg et al. (2002) model to extract a representation of muscle biomechanics from the known muscle activations (Fig. 1*B*). This was achieved by determining the set of pulling vectors, $\mathbf{P}_i$, that resulted in the best aiming performance, i.e., that minimizes endpoint errors, $E = \|\mathbf{x}_{targ} - \mathbf{x}\|^2$, when combined with the actual muscle activation, $\mathbf{a}$. To this end, we used a custom coordinate descent algorithm with the following steps. *1*) Assign random values to the initial set of pulling vectors in the physiological range of muscle force and direction. *2*) Pick a muscle at random and modify its pulling vector by changing its endpoint by a step in 4 orthogonal directions. The target errors associated with each of the 5 pulling vectors (i.e., the

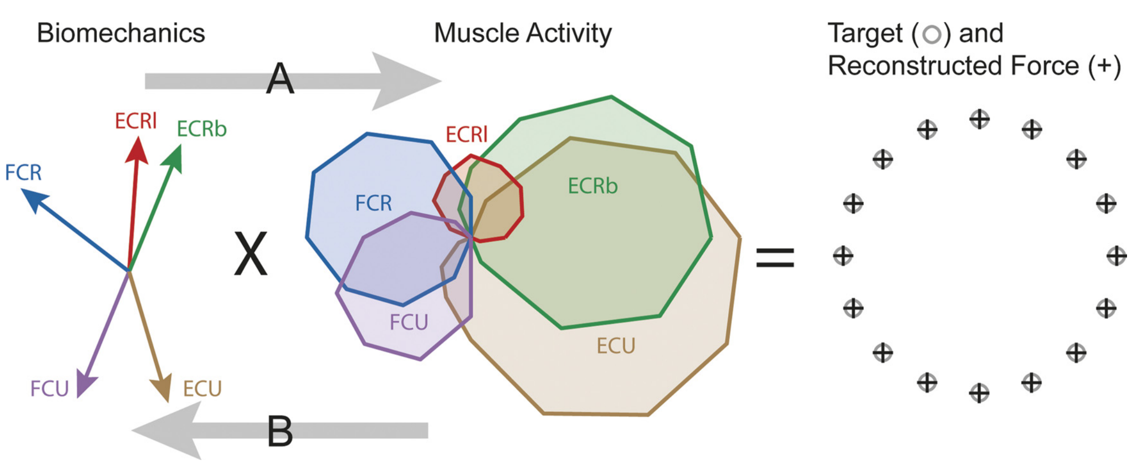

Fig. 1. Muscle biomechanics combined with muscle activity determine reaches to isometric force targets. *A*: Fagg et al. (2002) optimize muscle activity for the biomechanics of a given muscle. *B*: we use a similar optimization procedure in the opposite direction to determine the representation of muscle biomechanics (i.e., the muscle pulling vectors) that best reaches the force targets for a given pattern of muscle activities. ECRl, extensor carpi radialis longus; ECRb, extensor carpi radialis brevis; FCR, flexor carpi radialis; FCU, flexor carpi ulnaris; ECU, extensor carpi ulnaris.

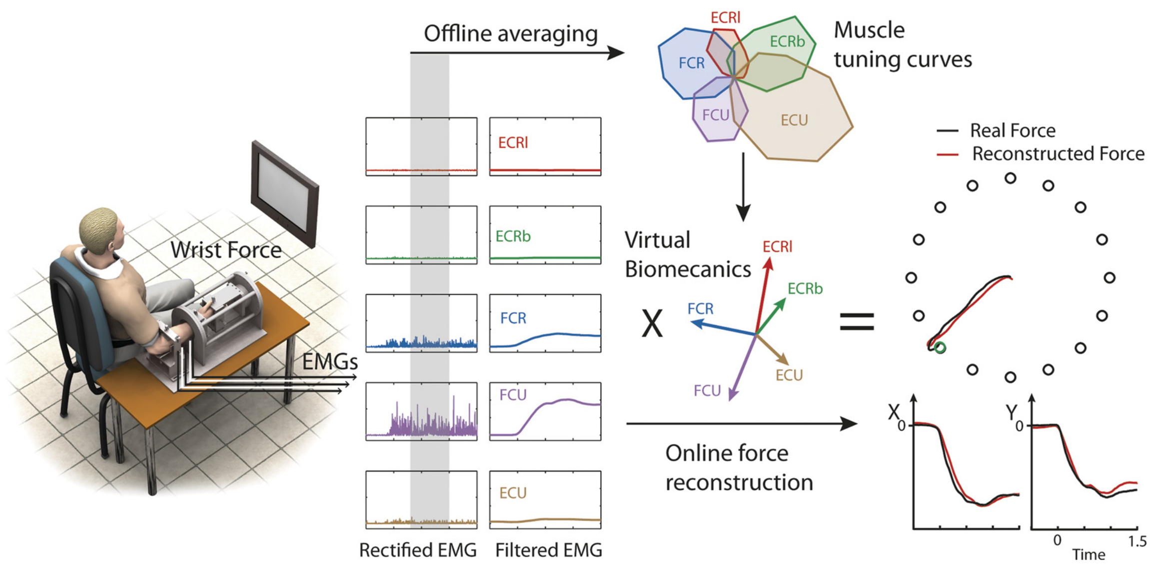

Fig. 2. Online force reconstruction from muscle virtual biomechanics and real-time electromyograms (EMGs). Subjects produced isometric force at the wrist to reach for 1 of 16 equally distributed target directions. Data from a force-driven condition in which the visual cursor represents the real isometric force are used to generate the time-independent patterns of muscle activation (i.e., the muscle tuning curves) used to extract the muscle pulling vectors (i.e., virtual biomechanics). Online force reconstruction is then obtained by multiplying the rectified filtered EMG signals to the pulling vector of each muscle. Note that EMG signals are shown from 1 trial only, whereas EMGs from 5 consecutive trials to each of the 16 targets are used to compute muscle tuning curves. Also note that for the purpose of illustration, the same EMG signals are used for offline averaging and online force reconstruction, whereas in the experiments, EMG for those 2 processes come from different acquisition blocks (i.e., in force-driven and EMG-driven conditions, respectively).

original and the 4 modified for that muscle) were then calculated as the summed squared error between targets and reconstructed reaches, and the pulling vector that produced the lowest cost was retained. *3*) One iteration of the model was said to be completed when each muscle had been optimized once. *4*) The whole model was iterated until the overall cost converged to a low value. For the steady-state isometric tasks presented here, an exact solution can be obtained by separate minimization of the squared horizontal and vertical errors using the ordinary least-squares method. For all subjects and experimental sessions reported, we have checked that the coordinate descent algorithm used successfully converged to the exact solution. The coordinate descent method will be necessary if the virtual biomechanical modeling method is extended to tasks involving nonlinear dynamic terms.

Online force reconstruction. Figure 2 illustrates how we used EMG recordings during isometric force production at the wrist to extract the virtual biomechanics as indicated previously and how it was combined with real-time EMG to reconstruct force online. To generate the time-independent patterns of muscle activation used to extract the virtual biomechanics, rectified EMG for each muscle was first averaged over the steady, holding phase of the force on target (i.e., during a time window from 300 to 1,000 ms after movement onset, while the task was to achieve force targets with a movement time between 150 and 250 ms, and to hold the force cursor on target for 1 s). As indicated later in this section, participants performed 6 consecutive reaches to each of the 16 targets, and averages over the 5 last reaches were used to compute the time-independent muscle tuning curves (i.e., 1st reach discarded). Once the virtual biomechanics were extracted, each pulling vector is simply multiplied by $a_i(t)$ and the resultants summed to generate the time course of the reconstructed force, $\widehat{\mathbf{F}(t)}$. The activation values $a_i(t)$ are assumed to be linearly related to the rectified and filtered (1.3-Hz low-pass) EMG signals, normalized to the largest EMG value obtained for each in a series of maximal voluntary contractions (MVC) in different directions (see below).

$$\widehat{\mathbf{F}(t)} = \sum_{i \in A} \mathbf{P}_i \, a_i(t)$$

Experiments

We tested our virtual biomechanics technique for online force reconstruction in different experimental context involving participants to reach isometric force targets in various directions. The technique was first evaluated with surface EMG (*experiment 1*, $n = 6$) and second with fine-wire electrodes (*experiment 2*, $n = 6$) with the forearm in a neutral posture (i.e., forearm midprone as displayed Fig. 2). Then, we tested the sensitivity of the technique to changes in biomechanics elicited by variation of the forearm orientation along the supination/pronation axis (*experiment 3*, $n = 6$). In all experiments, the real and reconstructed forces were compared during the reaching task performed with a visual cursor that represented the real force produced. EMG patterns observed in that context were also compared with EMG patterns produced when the reaching task was performed with online reconstructed force as the visual cursor.

Subjects. Twelve healthy, right-handed subjects (all men, age 23–38 yr) volunteered for this study. When subjects participated in more than one experiment ($n = 4$), testing sessions were separated by at least 3 wk. All subjects had normal or corrected-to-normal vision. They all gave informed written consent before the experiment, which was approved by the local ethics committee and conformed to the Declaration of Helsinki.

General experimental procedure. Subjects sat 80 cm from a computer display positioned at eye level. The right hand was maintained in a custom-made manipulandum with the forearm in one of three possible positions: in a neutral position for *experiments 1* and *2* (midway between pronation and supination as displayed Fig. 2) and in 80° pronation or −80° supination for *experiment 3*. The elbow was kept at 110° with the forearm parallel to the table and supported by a custom-built device similar to that used in a previous study (de Rugy and Carroll 2010). The wrist was fixed by an array of adjustable supports contoured to fit the hand at the metacarpal-phalangeal joints (12 contacts) and the wrist just proximal to the radial head (10 contacts). This allowed wrist forces to be applied without the need for a gripping force. Wrist forces were recorded using a 6-degrees-of-freedom force/torque transducer (45E15A-I63-A 400N60S; JR3, Woodland, CA) coupled with the wrist manipulandum.

Real-time visual feedback of either the real wrist forces or the reconstructed wrist forces was presented on the visual display. Targets were presented at 16 radial positions around the center of the display (i.e., 22.5° apart). In the neutral position, flexion/extension corresponded to the horizontal axis (flexion left), and radial/ulnar deviation corresponded to the vertical axis (radial deviation up). In the 2 other rotated forearm postures, the visual feedback was rotated with the forearm such that the movement of the cursor matched the force direction in external space.

In all experiments, a block of 32 MVC trials was 1st conducted for each subject with the forearm in the neutral posture. This block was used to normalize the activity of each muscle during the aiming task to the maximal EMG obtained in that muscle during MVC toward any target direction. Each of the 16 target directions was presented twice in a randomized order. For each direction, subjects were asked to raise their force rapidly to the maximal extent while maintaining the force direction within a delineated range of ±8° of target direction. Maximal forces were held for ~2 s. Fifteen seconds were allowed for rest before the next target appeared in another direction.

Each experiment contained "force-driven" block(s) in which the visual cursor used to reach targets represented the real force and "EMG-driven" blocks in which the cursor represented the reconstructed force. Each force-driven block consisted of 96 trials (6 trials for each of the 16 target directions) in which a low level of force (i.e., 22.5 N, which represents ~20% MVC for the subjects tested) was required to reach targets. This level of force was identical across all subjects and chosen to reduce the possibility of fatigue. Each trial began only if the cursor was maintained <5% of the target distance from the origin continuously for 200 ms. The origin was calibrated to 0 force along both axes (wrist relaxed) before each block. A random foreperiod (1–2 s) elapsed before a single target appeared coincident with a brief tone. Participants were asked to move the cursor to the target with a movement time of between 150 and 250 ms, defined as the time between 10 and 90% of the radial distance to the target, and to hold the cursor continuously for 1 s within the target zone (a trapezoid ±8° from target direction by 10% of radial distance to target). A high-pitched tone signaled that the target had been acquired. If the target was not acquired within 2 s of target presentation, a low-pitched tone indicated the end of the trial. A 2nd tone (200 ms after the 1st) indicated whether the movement time was correct (high tone) or not (low tone), and a bar graph provided visual feedback of the movement time in relation to the prescribed time window. Both the target and cursor disappeared at target acquisition or trial end, and ≥1 s elapsed before the start of the next trial. For each block, 6 consecutive trials were conducted for each 1 of 16 randomly ordered targets. EMG-driven blocks were identical to force-driven blocks with the only exception that the real force feedback was replaced by the reconstructed force.

In *experiments 1* and *2*, each participant performed one force-driven block immediately followed by an EMG-driven block. In *experiment 3*, participants performed the same 2 blocks but both in the pronated posture and in the supinated posture (4 blocks total).

EMG procedures. Bipolar EMG signals were recorded from extensor carpi radialis longus (ECRl), extensor carpi radialis brevis (ECRb), flexor carpi radialis (FCR), flexor carpi ulnaris (FCU), and extensor carpi ulnaris (ECU) muscles either with self-adhesive surface electrodes (*experiment 1*, 12-mm diameter recording surface, 2-cm interelectrode distance) or with fine-wire intramuscular electrodes (*experiments 2* and *3*, 75-μm diameter, 2 mm stripped from insulation for recording sites, single wires inserted at 1.5-cm interelectrode distance, dipole axes approximately parallel to the long axis of muscles). Signals were band-pass filtered from 30 Hz to 1 kHz, amplified 200–5,000 times (P511; Grass Instrument, Astro-Med, West Warwick, RI), and sampled at 2 kHz. Electrode locations were determined according to procedures previously reported (Selvanayagam et al. 2011).

Data reduction and analysis. Muscle tuning curves, or the time-independent muscular activity as a function of target direction, were determined for each muscle as the mean rectified EMG during the hold phase of the task (i.e., in a time window from 300 to 1,000 ms after movement onset) averaged over 5 trials to each target (the 1st of the 6 consecutive trials to each target was discarded to prevent the uncertainty about target direction from contaminating the data).

The spatiotemporal match between the real and reconstructed forces, or the goodness of force reconstruction, was quantified by defining a multivariate r^2 similar to that used in d'Avella et al. (2006):

$$r^2 = 1 - \frac{\text{SSE}}{\text{SST}} = 1 - \frac{\sum_{j \in M} \sum_{t \in N} \|\boldsymbol{F}(t) - \widehat{\mathbf{F}(t)}\|^2}{\sum_{j \in M} \sum_{t \in N} \|\boldsymbol{F}(t) - \overline{\boldsymbol{F}}\|^2}$$

where SSE is the sum of the squared residuals, SST is the sum of the squared residual from the mean force vector ($\overline{\mathbf{F}}$), M is the set of trials in a block, and N is the set of time samples per trials. Note that with this calculation, negative values of r^2 might occur with particularly poor force reconstruction (i.e., if SSE > SST).

To test specific hypothesis, the goodness of force reconstruction was computed in four instances after using alternate methods of force reconstruction. In *experiment 1*, force was additionally reconstructed using a set of virtual pulling vectors computed while completely ignoring either one or two muscles. When ignoring one muscle, each of the five muscles was selectively ignored (i.e., only our pulling vectors determined that best reach the targets), and the goodness of force reconstruction was averaged over the five combinations of one muscle ignored. When ignoring two muscles, all possible pairs of two muscles were considered, and the goodness of force reconstruction was averaged over all combinations. In *experiment 1*, force was also reconstructed using a set of virtual pulling vectors constrained by morphometric data from cadaver (Loren et al. 1996). Specifically, the directions and relative magnitudes of the pulling vectors were fixed according to data from Loren et al. (1996), and the overall magnitude only was optimized to reach best the targets when combined with muscle activities recorded for each subject. This was designed to compare our method with force reconstructed using a realistic biomechanical model of the wrist. In *experiment 4*, force was additionally reconstructed using the set of virtual pulling vectors extracted from muscle tuning curves obtained in the other forearm posture. This was designed to ascertain that our reconstruction method is sensitive to biomechanical changes elicited by the different postures. Differences between goodness of force reconstruction obtained for different experiments were tested using independent-samples *t*-tests, and differences between goodness of force reconstruction from different reconstruction methods within the same experiment were tested using paired-samples *t*-tests.

In *experiments 1* and *2*, the time-independent pattern of muscle activities (i.e., muscle activity averaged per target direction) were analyzed using 3-way repeated-measures ANOVAs [2 feedback conditions (force-driven vs. EMG-driven) × 5 muscles × 16 directions of force targets]. In *experiment 3*, a 4-way repeated-measures ANOVA was conducted using posture (pronation vs. supination) as an additional factor. The significance level was set to $\alpha = 0.05$.

RESULTS

Surface EMG: Experiment 1

The force reconstructed with our virtual biomechanics on the EMG-driven blocks of this experiment explained 92.0% of the variance of the real force signals (i.e., $r^2 = 0.920 \pm 0.035$, mean ± SD). Figure 3 illustrates that this proportion of explained variance deteriorates when the technique is applied with one missing muscle ($t = 15.34$, $P < 0.0005$; $r^2 = 0.671 \pm$

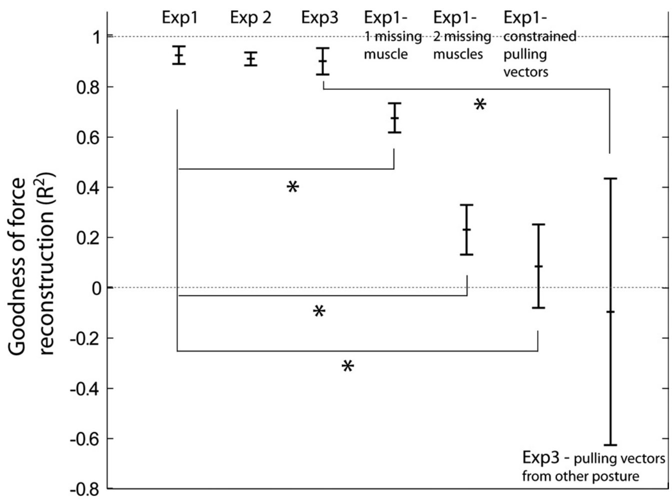

Fig. 3. Goodness of force reconstruction (r^2) for the 3 different experiments (Exp) and for the 4 alternate force reconstruction methods: with the pulling vectors computed while ignoring either 1 or 2 muscles for *experiment 1*, with the pulling vectors constrained by a realistic biomechanical model for *experiment 1*, and using the set of pulling vectors extracted from the other posture for *experiment 3* (cf. main text). Error bars represent standard deviations, and significant differences are indicated by asterisks ($P < 0.05$).

0.058) and with two missing muscles ($t = 20.76$, $P < 0.0005$; $r^2 = 0.226 \pm 0.098$). This is likely due to the fact that there is relatively low mechanical redundancy at the wrist joint and, consequently, that a representation of the biomechanics of all muscles is necessary to produce reasonable force reconstruction.

Figure 3 also illustrates that this proportion of explained variance is in marked contrast ($t = 12.34$, $P < 0.0005$) with that obtained when force is reconstructed with an EMG-driven biomechanical model that conforms to measurement from cadaver (i.e., $r^2 = 0.082 \pm 0.165$). Figure 4 further illustrates how the goodness of the force reconstruction was dramatically affected when the muscle virtual pulling vectors were constrained. When the pulling vectors were unconstrained, the set of vectors (Fig. 4*B*) that best reached the target produced accurate reaches (Fig. 4*C*) when combined with the muscle tuning curves (Fig. 4*A*). When combined online with EMG in an EMG-driven block, this set of vectors also enables a close match between real force (Fig. 4*F*) and reconstructed force (Fig. 4*G*). However, when the set of pulling vectors were constrained in direction and relative magnitude by biomechanical data from cadavers (Fig. 4*C*), the reconstructed reach was poor (Fig. 4*E*), which also translated in poor reconstructed force (Fig. 4*H*).

Figure 5*A* illustrates for a representative subject that muscle tuning curves obtained in EMG-driven condition, where the feedback represented the reconstructed force, are very similar to those obtained in force-driven condition (i.e., real force feedback). The repeated-measures ANOVA on averaged EMG during the hold phase of the task revealed a strong interaction between muscles and direction of force targets [$F(60, 300) = 47.96$, $P < 0.0005$] but no feedback conditions × muscles × directions interaction [$F(60, 300) = 1.16$, $P = 0.21$]. This indicated that muscle tuning curves could not be distinguished between force-driven and EMG-driven conditions when the technique was applied with surface EMG.

Fine-Wire EMG: Experiment 2

When the technique was applied with fine-wire recordings, the EMG-based force reconstruction explained 90.5% of the variance of the real force signals (i.e., $r^2 = 0.905 \pm 0.026$). This proportion of explained variance is similar ($t = 0.85$, $P = 0.439$) to that obtained with surface electrodes in *experiment 1*. Figure 5*B* also illustrates that as for surface recordings, the technique applied with fine-wire recording produces muscle tuning curves that match well between force-driven and EMG-driven conditions. As for *experiment 1*, the repeated-measures ANOVA revealed strong muscles × directions interaction [$F(60, 300) = 40.87$, $P < 0.0005$] but no feedback conditions × muscles × directions interaction [$F(60, 300) = 1.28$, $P = 0.09$], indicating strong muscular tuning that is similar for force-driven and EMG-driven conditions.

Sensitivity to Biomechanical Changes with Forearm Posture: Experiment 3

When we tested the sensitivity of the technique to changes in biomechanics elicited by changes in posture, we found that the EMG-based force reconstruction applied to the two different forearm postures tested explained 89.5% of the variance of the real force signals (i.e., $r^2 = 0.895 \pm 0.052$). This proportion of explained variance is very different ($t = 6.78$, $P < 0.0005$) from that obtained when force is reconstructed for a given posture (e.g., pronation) with the set of pulling vectors extracted from the other posture (e.g., supination; $r^2 = 0.099 \pm 0.529$). Figure 6 illustrates for a representative subject that muscle tuning curves were markedly different for the task performed in supination and in pronation but very similar between force-driven and EMG-driven conditions. The repeated-measures ANOVA revealed strong muscles × directions interaction [$F(60, 300) = 43.79$, $P < 0.0005$], a strong postures × muscles × directions interaction [$F(60, 300) = 11.93$, $P < 0.0005$], but no feedback conditions × postures × muscles × directions interaction [$F(60, 300) = 1.23$, $P = 0.13$]. This indicates that muscle tuning curves were strongly tuned to the directions of force targets, that this tuning was different for the two different postures, but could not be distinguished between force-driven and EMG-driven conditions.

DISCUSSION

Our goal was to develop a technique that enables accurate online force reconstruction from imperfect EMG recordings. Instead of seeking an accurate biomechanical model, we employed an alternative, practical approach whereby a virtual representation of muscle biomechanics is defined that best reconstructs force when combined with available EMG recordings. The virtual biomechanics method was applied during two-dimensional isometric force at the wrist in a controlled musculoskeletal configuration that restricted changes in muscle length and moment arm. We demonstrated that the technique works for various experimental contexts in which we varied the recordings methods as well as the muscle biomechanics. This method assumes a linear relationship between muscle activation and rectified EMG, which is likely to be true for the relatively small range of isometric forces produced by our subjects in this task.

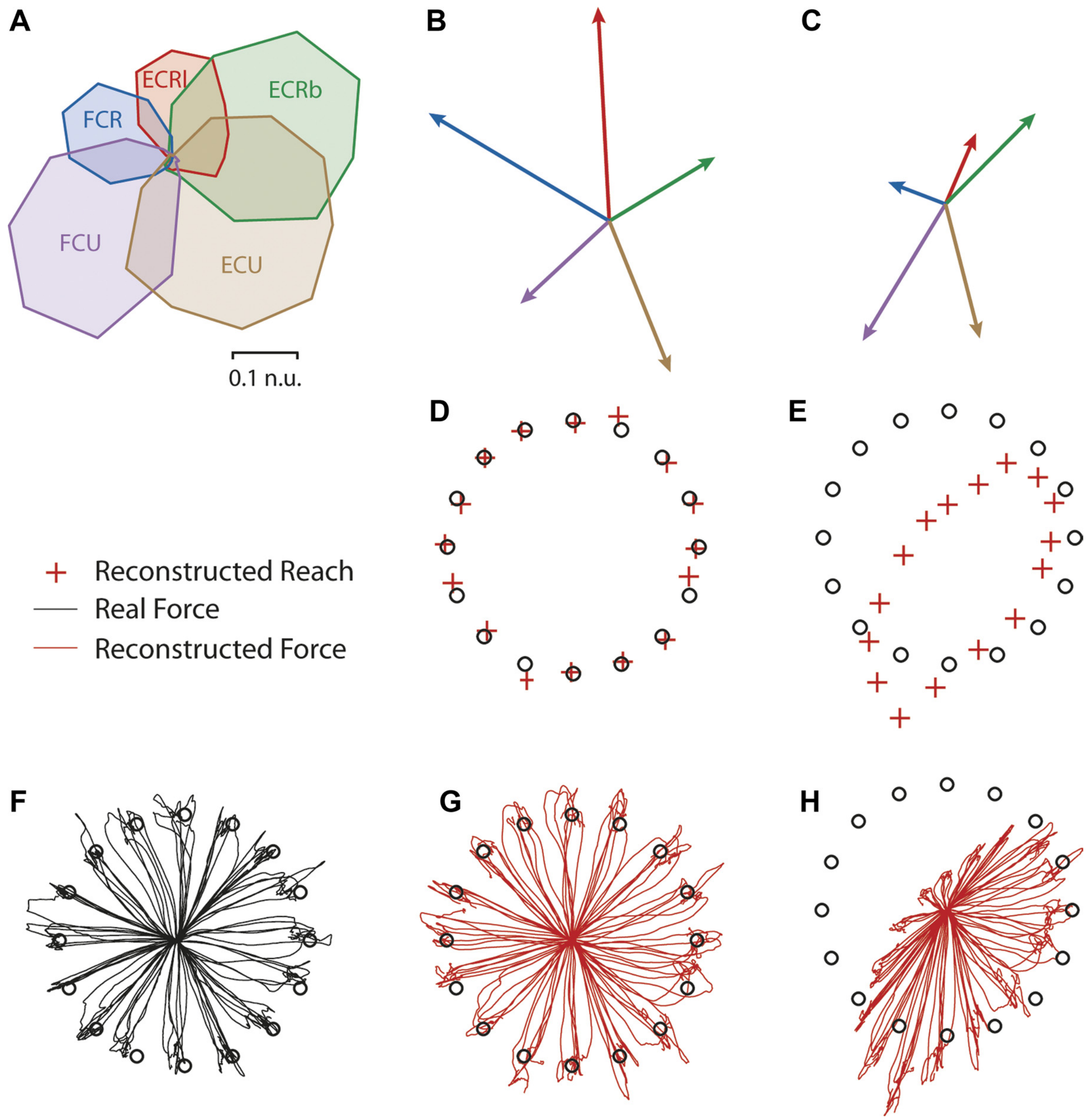

Fig. 4. Illustration of the deterioration of force reconstruction when the pulling vectors were constrained in direction and magnitude by biomechanical data. *A*: muscle tuning curve. *B*: pulling vectors freely determined. *C*: constrained pulling vectors. *D* and *E*: reconstructed reaches with unconstrained (*E*) and constrained (*F*) vectors. *F*: real force. *G* and *H*: reconstructed forces with unconstrained (*G*) and constrained (*H*) vectors. Data from this figure come from an EMG-driven block of the subject who obtained the highest goodness of force reconstruction ($r^2 = 0.28$) with the constrained vectors.

Robustness to Limitations from EMG Recordings

Two major issues associated with EMG recordings are cross talk and representativeness (Hug 2011; Staudenmann et al. 2010). Cross talk refers to a contamination of EMG signals by electrical activity of nearby muscles, and representativeness refers to the proportion of active motor units captured by the signal. Because electrodes are directly inserted into the target muscle, fine-wire recordings are less subject to cross talk than surface recordings that are more remote and less precisely positioned relative to muscles (Selvanayagam et al. 2012). Fine-wire recordings, however, are more selective to the part of the muscle into which the electrodes are inserted and therefore less representative of the overall activity of the target muscle. By showing that our technique works equally well with both types of recordings, we demonstrated that it is robust to both of their associated limitations. It is worth noting that both cross talk and selective sampling of muscle fibers in the vicinity of the electrodes would affect force reconstructions using forward simulations of an accurate biomechanical model. Although these limitations could be substantially reduced using high-density EMG (Staudenmann et al. 2010), our reconstruction method obviates the need for this technology, which would be expensive and demanding to incorporate the multiple muscles needed for force reconstruction in various directions as achieved here.

Sensitivity to Biomechanical Changes with Posture

As muscle length and moment arms change with musculoskeletal configuration, so changes the torque generation of muscles and therefore the muscle activation patterns capable of

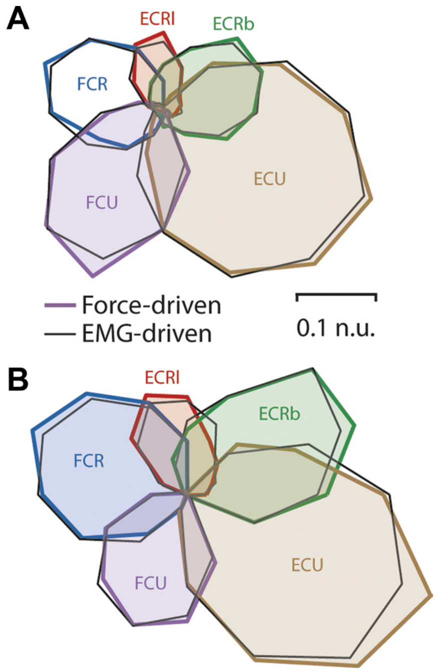

Fig. 5. Example of muscle tuning curves obtained in force-driven condition and in EMG-driven condition for the same subject in *experiment 1* (*A*; surface EMG) and in *experiment 2* (*B*; fine-wire EMG). EMG activities are normalized to maximal EMG, and a scale bar indicates 0.1 normalized units (n.u.).

generating a given joint torque in a given posture. How the nervous system adjusts motor commands to the biomechanics of the current posture is a key problem of motor control, which has been explored by simultaneously assessing changes in muscle biomechanics, in muscle activities, and in neural activities at various levels of the CNS (Buneo et al. 1997; Kakei et al. 1999, 2001; Sergio and Kalaska 1997, 2003; Yanai et al. 2008). For instance, nonhuman primate studies reported systematic changes in muscle activity selected to produce force at the wrist in different forearm orientation (Kakei et al. 1999, 2001). In a recent study in which we assessed these changes in humans, we showed in particular that FCR displayed higher activity and broader tuning during force produced with the forearm in a pronated position compared with a supinated position (de Rugy et al. 2012a). A similar pattern is visible in our data displayed Fig. 5 that has also been replicated in our condition in which the task was controlled with force reconstructed from EMG instead of real force. We therefore demonstrated that our force reconstruction technique fully captures biomechanical changes associated with the different forearm postures. This is important because it means that we can use this technique to address the question of how the nervous system tunes motor commands to the biomechanics of the current posture. In fact, we have recently addressed this question by simulating the biomechanics of a different posture to show that participants initially compensate for this perturbation using a linear scaling of their original pattern of muscle activity (i.e., the pattern that corresponds to the real posture; de Rugy et al. 2012b).

Potential Contributions from Hand and Finger Muscles

The current force reconstruction technique has ignored potential contributions from the numerous (i.e., 19) hand and finger muscles that cross the wrist and that have nonnegligible moment arms in wrist flexion/extension and radial/ulnar deviation (e.g., see Fig. 3 in Gonzalez et al. 1997 for a visual representation of these moment arms at the wrist). We believe that the contribution from these muscles to the task was not high at the relatively low level of force involved here (i.e., ~20% MVC). This is because in our device the hand was fitted at the metacarpal-phalangeal joints such that the fingers were hanging in the air with no mechanical contact to the device and subjects were instructed to prevent any forcing or gripping that could bring the fingers in contact with the device. In this context, transmission of force from finger and hand muscles to the device is still possible through cocontraction that would maintain steady finger positions. Cocontractions between opposing finger extensors and flexors would be typically paralleled by opposing wrist extension and flexion moments, thereby reducing the net contribution at the wrist joint. However, the pulling vector discrepancies with respect to the anatomically constrained model appear to involve mostly underrepresented radial torques (see Fig. 4), which are particularly large for thumb extensors and flexors (Gonzalez et al. 1997). To rule out such a contribution, it would be necessary to obtain selective EMGs from at least a representative sampling of the thumb and finger muscles uncontaminated by cross talk from the nearby and simultaneously active wrist muscles. To incorporate such contributions into the model, it would be necessary to obtain quantitative EMGs from all 19 of these muscles during both their maximal activation and a sufficiently rich set of tasks for which their activity would be differentiated. Thus it is important to recognize that the virtual biome-

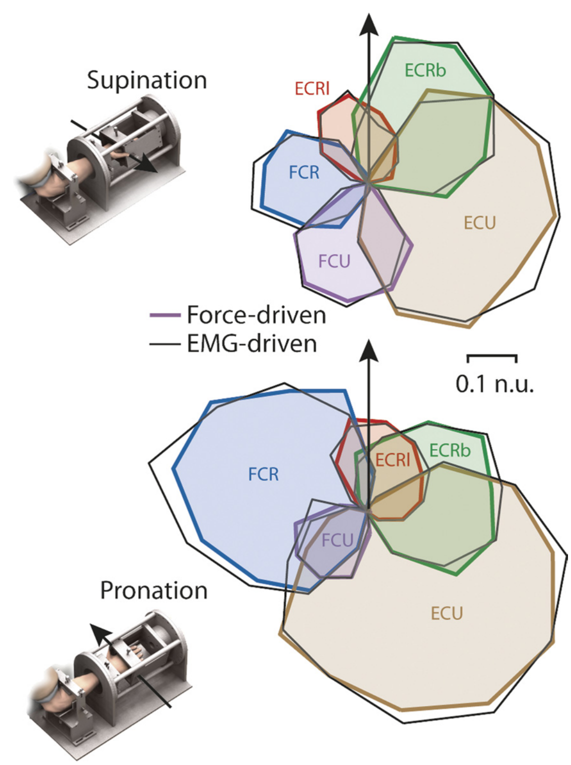

Fig. 6. Example of muscle tuning curves obtained in force-driven condition and in EMG-driven condition for 2 postures (i.e., −80° supination and +80° pronation) of 1 subject in *experiment 3*. The arrows indicate the wrist direction used for reference (i.e., radial deviation). EMG activities are normalized to maximal EMG, and a scale bar indicates 0.1 n.u.

chanical model is not intended to generate an accurate representation of the work of specific anatomical muscles. It is intended to provide a useful experimental tool to understand sensorimotor adaptation and learning when studied within the context of a well-defined task and subject-specific parameterization of the model. The robust quality of the force reconstructions presented here suggests that this goal has been met.

Differences with Existing EMG-Based Force Reconstruction

Our method is related to a previous method whereby coefficients that relate EMG to force are determined for individual muscles from a data set that requires production of force in various directions and knowledge of muscle moment arms (An et al. 1983; Buchanan et al. 1993; Messier et al. 1971). This approach, termed "coefficient methods" (Buchanan et al. 1993), would be similar to the method described here had we optimized only the magnitude of the muscle pulling vectors, i.e., by constraining the vector directions according to biomechanical data. A drawback of this method is that it implies knowledge of muscle moment arms, which requires magnetic resonance imaging to be accurately assessed on an individual basis (Buchanan et al. 1993). Kutch et al. (2010) recently proposed an alternative method based on surface EMG to extract the direction of action of finger muscles. However, this method might require EMG that represents accurately the activity of the overall muscle, as can be the case with finger muscles, since we were not able to generate reliable direction of action using this method for wrist muscles. In the end, muscle direction of action was unnecessary as our method is free of a priori biomechanical knowledge. We believe that this enabled additional flexibility that was beneficial to the high correlation obtained between forces reconstructed online and real forces.

Another related method was recently proposed whereby a matrix factorization algorithm is applied to surface EMG to extract control signals for prostheses (Jiang et al. 2009; see also Kamavuako et al. 2012). Using forces at the wrist as control signals and a generative model of surface EMG that assumes hard-wired muscle synergies, Jiang et al. (2009) obtained a goodness of force reconstruction that was comparable with that of the present experiments in the absence of simulated muscle cross talk (90.2% variance of the force signals explained) and that degraded with the level of cross talk. In an experiment using eight pairs of recording electrodes arbitrarily placed (equally spaced) around the forearm, they obtained a variance of force signals explained that dropped to 77.5%. The method presented here uses EMG signals that can be identified with specific muscles but compensates for their inevitable shortcomings of selectivity and sampling. This resulted in low residual errors for predicted force as well as the ability to simulate specific changes in musculoskeletal function in virtual force experiments. Neither the matrix factorization algorithm nor the probabilistic method of Seifert and Fuglevand (2002) would be suitable for this application.

Adaptation to Novel Virtual Biomechanics

Over the last few decades, the literature on sensorimotor adaptation has been dominated by two main classes of perturbations: force-field, whereby a force is applied to an end-effector, and sensorimotor shifts, such as in prism adaptation or visuomotor rotation (de Rugy et al. 2009; Gandolfo et al. 1996; Ghilardi et al. 1995; Shadmehr and Mussa-Ivaldi 1994; Shadmehr and Wise 2005; Simani et al. 2007; Welch et al. 1974). The present technique offers opportunities to study adaptation to a new class of perturbation, whereby the virtual biomechanics that link muscle activity to reconstructed force can be modified at will. In particular, this technique enables selective manipulation of properties of individual muscles that is not possible within the broad alteration of sensorimotor mapping induced by force fields or sensorimotor shifts. We have already used the technique to simulate the muscle-specific biomechanics of a different posture as well as the complete loss of a muscle and large amounts of signal-dependent noise added to a muscle (de Rugy et al. 2012b). In all of these conditions, we found that participants compensated for the perturbation using a linear scaling of their original pattern of muscle activity. This has important implications because, although the pattern of muscle activity used to produce force at the wrist is reasonably well-reproduced by optimization models (Diedrichsen et al. 2010; Fagg et al. 2002; Haruno and Wolpert 2005), how the nervous system achieves this behavior remains largely unresolved. For instance, our previous results appear inconsistent with online optimization of muscle activities, as this should have elicited a reoptimization that was not observed when faced to conditions of novel biomechanics. Instead, the observed scaling of the original pattern suggests an important role of the lower sensorimotor circuitry, which might not be readily available to adaptation. Although these results hold only for the brief time scale tested so far, the method presented here could in principle be used to assess adaptation over much longer time scales.

The force reconstruction method allows modifications of the virtual biomechanics that are limited only by imagination. For instance, one might take advantage of the facts that wrist muscles switch their functional relationship depending on the direction of action and that the spinal cord circuitry is known to be intimately related to this adjustable functional relationship (Pierrot-Deseilligny and Burke 2005; Raphael et al. 2010). During wrist extension, the extensor muscles function as agonists, and the flexor muscles function as antagonists, but during radial/ulnar deviation, the extensor muscles (as well as the flexor muscles) oppose each other. Adjacent muscles could therefore be considered as "partial synergists" because they switch from agonist to antagonist based on the direction of action, and diagonal muscles that are farthest apart from each other as "true antagonists" because they always oppose each other (for example, FCR and ECU). The implication of this functional organization on sensorimotor adaptation could be tested using the virtual biomechanics to simulate different arrangements of muscles that would vary the degree of integrity of their functional relationships. Importantly, the current technique has the potential to start from the most intuitive relationship between muscle activity and force (i.e., the natural relationship) before introducing modifications. Myoelectric controllers for prosthetic limbs typically aim for intuitive mappings to reduce learning requirements (Hargrove et al. 2009; Parker et al. 2006; Zhou et al. 2007). However, Radhakrishnan et al. (2008) reported that learning a novel nonintuitive arrangement was more feasible when it involved muscles that were less functionally related. The technique presented here offers new opportunities to explore these issues.

DISCLOSURES

No conflicts of interest, financial or otherwise, are declared by the author(s).

AUTHOR CONTRIBUTIONS

A.d.R., G.E.L., and T.J.C. conception and design of research; A.d.R. and T.J.C. performed experiments; A.d.R. and T.J.C. analyzed data; A.d.R., G.E.L., and T.J.C. interpreted results of experiments; A.d.R. prepared figures; A.d.R. drafted manuscript; A.d.R., G.E.L., and T.J.C. edited and revised manuscript; A.d.R., G.E.L., and T.J.C. approved final version of manuscript.

REFERENCES

An KN, Cooney WP, Chao EY, Askew LJ, Daube JR. Determination of forces in extensor pollicis longus and flexor pollicis longus of the thumb. *J Appl Physiol* 54: 714–719, 1983.

Bernstein NA. *The Coordination and Regulation of Movements*. Oxford, UK: Pergamon Press, 1967.

Buchanan TS, Lloyd DG, Manal K, Besier TF. Neuromusculoskeletal modeling: estimation of muscle forces and joint moments and movements from measurements of neural command. *J Appl Biomech* 20: 367–395, 2004.

Buchanan TS, Moniz MJ, Dewald JP, Zev RW. Estimation of muscle forces about the wrist joint during isometric tasks using an EMG coefficient method. *J Biomech* 26: 547–560, 1993.

Buneo CA, Soechting JF, Flanders M. Postural dependence of muscle actions: implications for neural control. *J Neurosci* 17: 2128–2142, 1997.

Cheng EJ, Loeb GE. On the use of musculoskeletal models to interpret motor control strategies from performance data. *J Neural Eng* 5: 232–253, 2008.

d'Avella A, Portone A, Fernandez L, Lacquaniti F. Control of fast-reaching movements by muscle synergy combinations. *J Neurosci* 26: 7791–7810, 2006.

d'Avella A, Saltiel P, Bizzi E. Combinations of muscle synergies in the construction of a natural motor behavior. *Nat Neurosci* 6: 300–308, 2003.

de Rugy A, Carroll TJ. Changes in muscle directional tuning parallel feedforward adaptation to a visuomotor rotation. *Exp Brain Res* 203: 701–709, 2010.

de Rugy A, Davoodi R, Carroll TJ. Changes in wrist muscle activity with forearm posture: Implications for the study of sensorimotor transformations. *J Neurophysiol*. First published September 12, 2012a, doi:10.1152/jn.00130.2012.

de Rugy A, Hinder MR, Woolley DG, Carson RG. The synergistic organization of muscle recruitment constrains visuomotor adaptation. *J Neurophysiol* 101: 2263–2269, 2009.

de Rugy A, Loeb GE, Carroll TJ. Muscle coordination is habitual rather than optimal. *J Neurosci* 32: 7384–7391, 2012b.

Diedrichsen J, Shadmehr R, Ivry RB. The coordination of movement: optimal feedback control and beyond. *Trends Cogn Sci* 14: 31–39, 2010.

Erdemir A, McLean S, Herzog W, van den Bogert AJ. Model-based estimation of muscle forces exerted during movements. *Clin Biomech (Bristol, Avon)* 22: 131–154, 2007.

Fagg AH, Shah A, Barto AG. A computational model of muscle recruitment for wrist movements. *J Neurophysiol* 88: 3348–3358, 2002.

Gandolfo F, Mussa-Ivaldi FA, Bizzi E. Motor learning by field approximation. *Proc Natl Acad Sci USA* 93: 3843–3846, 1996.

Ghilardi MF, Gordon J, Ghez C. Learning a visuomotor transformation in a local area of work space produces directional biases in other areas. *J Neurophysiol* 73: 2535–2539, 1995.

Gonzalez RV, Buchanan TS, Delp SL. How muscle architecture and moment arms affect wrist flexion-extension moments. *J Biomech* 30: 705–712, 1997.

Hargrove LJ, Li G, Englehart KB, Hudgins BS. Principal components analysis preprocessing for improved classification accuracies in pattern-recognition-based myoelectric control. *IEEE Trans Biomed Eng* 56: 1407–1414, 2009.

Haruno M, Wolpert DM. Optimal control of redundant muscles in step-tracking wrist movements. *J Neurophysiol* 94: 4244–4255, 2005.

Hug F. Can muscle coordination be precisely studied by surface electromyography? *J Electromyogr Kinesiol* 21: 1–12, 2011.

Jiang N, Englehart KB, Parker PA. Extracting simultaneous and proportional neural control information for multiple-DOF prostheses from the surface electromyographic signal. *IEEE Trans Biomed Eng* 56: 1070–1080, 2009.

Kakei S, Hoffman DS, Strick PL. Muscle and movement representations in the primary motor cortex. *Science* 285: 2136–2139, 1999.

Kakei S, Hoffman DS, Strick PL. Direction of action is represented in the ventral premotor cortex. *Nat Neurosci* 4: 1020–1025, 2001.

Kamavuako EN, Englehart KB, Jensen W, Farina D. Simultaneous and proportional force estimation in multiple degrees of freedom from intramuscular EMG. *IEEE Trans Biomed Eng* 59: 1804–1807, 2012.

Kutch JJ, Kuo AD, Rymer WZ. Extraction of individual muscle mechanical action from endpoint force. *J Neurophysiol* 103: 3535–3546, 2010.

Loeb GE, Brown IE, Cheng EJ. A hierarchical foundation for models of sensorimotor control. *Exp Brain Res* 126: 1–18, 1999.

Loren GJ, Shoemaker SD, Burkholder TJ, Jacobson MD, Friden J, Lieber RL. Human wrist motors: biomechanical design and application to tendon transfers. *J Biomech* 29: 331–342, 1996.

Messier RH, Duffy J, Litchman HM, Paslay PR, Soechting JF, Stewart PA. The electromyogram as a measure of tension in the human biceps and triceps muscles. *Int J Mech Sci* 13: 585–598, 1971.

Parker P, Englehart K, Hudgins B. Myoelectric signal processing for control of powered limb prostheses. *J Electromyogr Kinesiol* 16: 541–548, 2006.

Pierrot-Deseilligny E, Burke D. *The Circuitry of the Human Spinal Cord, its Role in Motor Control and Movement Disorders*. Cambridge, UK: Cambridge Univ. Press, 2005.

Radhakrishnan SM, Baker SN, Jackson A. Learning a novel myoelectric-controlled interface task. *J Neurophysiol* 100: 2397–2408, 2008.

Raphael G, Tsianos GA, Loeb GE. Spinal-like regulator facilitates control of a two-degree-of-freedom wrist. *J Neurosci* 30: 9431–9444, 2010.

Sartori M, Reggiani M, van den Bogert AJ, Lloyd DG. Estimation of musculotendon kinematics in large musculoskeletal models using multidimensional B-splines. *J Biomech* 45: 595–601, 2012.

Seifert HM, Fuglevand AJ. Restoration of movement using functional electrical stimulation and Bayes' theorem. *J Neurosci* 22: 9465–9474, 2002.

Selvanayagam VS, Riek S, Carroll TJ. A systematic method to quantify the presence of cross-talk in stimulus-evoked EMG responses: implications for TMS studies. *J Appl Physiol* 112: 259–265, 2012.

Selvanayagam VS, Riek S, Carroll TJ. Early neural responses to strength training. *J Appl Physiol* 111: 367–375, 2011.

Sergio LE, Kalaska JF. Systematic changes in directional tuning of motor cortex cell activity with hand location in the workspace during generation of static isometric forces in constant spatial directions. *J Neurophysiol* 78: 1170–1174, 1997.

Sergio LE, Kalaska JF. Systematic changes in motor cortex cell activity with arm posture during directional isometric force generation. *J Neurophysiol* 89: 212–228, 2003.

Shadmehr R, Mussa-Ivaldi FA. Adaptive representation of dynamics during learning of a motor task. *J Neurosci* 14: 3208–3224, 1994.

Shadmehr R, Wise SP. *The Neurobiology of Reaching and Pointing*. Cambridge, MA: MIT Press, 2005.

Simani MC, McGuire LM, Sabes PN. Visual-shift adaptation is composed of separable sensory and task-dependent effects. *J Neurophysiol* 98: 2827–2841, 2007.

Staudenmann D, Roeleveld K, Stegeman DF, van Dieën JH. Methodological aspects of SEMG recordings for force estimation–a tutorial and review. *J Electromyogr Kinesiol* 20: 375–387, 2010.

Todorov E. Optimality principles in sensorimotor control. *Nat Neurosci* 7: 907–915, 2004.

Todorov E, Jordan MI. Optimal feedback control as a theory of motor coordination. *Nat Neurosci* 5: 1226–1235, 2002.

Tsianos GA, Rustin C, Loeb GE. Mammalian muscle model for predicting force and energetics during physiological behaviors. *IEEE Trans Neural Syst Rehabil Eng* 20: 117–133, 2012.

Welch RB, Choe CS, Heinrich DR. Evidence for a three-component model of prism adaptation. *J Exp Psychol* 103: 700–705, 1974.

Yanai Y, Adamit N, Israel Z, Harel R, Prut Y. Coordinate transformation is first completed downstream of primary motor cortex. *J Neurosci* 28: 1728–1732, 2008.

Zhou P, Lowery MM, Englehart KB, Huang H, Li G, Hargrove L, Dewald JP, Kuiken TA. Decoding a new neural machine interface for control of artificial limbs. *J Neurophysiol* 98: 2974–2982, 2007.